Development of Graph Neural Network Interatomic Potential to Investigate Diamond Oxidation and Graphitization

John Isaac G. Enriquez and Yoshitada Morikawa

Osaka University Graduate School of Engineering

1. Introduction

Synthetic diamond has been regarded as an ideal material for several new technologies, particularly in high-power electronics and quantum devices [1,2]. The device fabrication methods used in conventional materials such as silicon are ineffective for diamond because of diamond's extreme hardness and chemical inertness. Plasma and thermochemical etching are currently used to fabricate diamond devices, though these technologies are arguably still in their infancy [3,4]. Understanding the diamond's oxidation, thermal degradation, and wear will lead to insights that scientists and engineers could use to accelerate the development diamond device fabrication methods.

While ab-initio methods have been useful in elucidating the surface chemistry and engineering design of materials, the high computational cost limits its application to small and highly idealized models. Recently, machine learning molecular dynamics (MLMD) simulation method has been gaining popularity. In this method, an analytic expression of the potential energy surface and its derivatives as a function of atomic positions is obtained by fitting onto ab-initio calculation results to perform simulations. The fitting procedure is performed using several machine learning and neural network methods, among which includes Gaussian process regression, high-dimensional neural network, and graph neural network. Successful construction of machine learning interatomic potentials (MLIP) will enable large scale and long timescale simulations with accuracies comparable to ab-initio molecular dynamics.

In this article, we discuss the method that we used in the construction of MLIP for the study of diamond oxidation, graphitization, and wear. In addition, we present some tools that we developed for the analysis of molecular dynamics simulation results.

2. Computational Details

A database of structures with total energy and forces is built using spin polarized density functional theory calculations with generalized gradient approximation exchange correlation functional. Semi empirical van der Waals correction is implemented. The core electrons were treated with ultrasoft pseudopotentials. The wave functions and augmentation charge are expanded using plane wave basis with cutoffs of 36 Ry (490 eV) and 400 Ry (5442 eV), respectively. Special points for Brillouin-zone integration were generated using the Monkhorst-Pack scheme. The convergence threshold for energy minimization is 1.0×10^{-9} Ha/atom (2.72×10^{-8} eV/atom). We perform geometry optimizations until the forces on each atom is less than 1.0×10^{-3} Ha/a_0 (5.14×10^{-2} eV/Å). The number of k-points depends on the simulation cell size and were all tested for convergence. All calculations were performed using the STATE code package [5].

The graph neural network interatomic potential is constructed using the Neural Equivariant Interatomic Potential (NequIP) software package [6]. This method implements graph message passing algorithm analogous to the convolution filters used in image recognition neural network models to generate equivariant representations of atomic environment. The message passing captures many-body interactions between atomic species. Molecular dynamics simulations are performed on LAMMPS code using an NVT ensemble with Nose-Hoover thermostat [7].

3. Results

3.1. Graph Neural Network Interatomic Potential Construction, Fine-tuning, and Evaluation

An initial database is constructed which is composed of equilibrium structures of diamond, graphite, graphene, and diamond (111) and (100) surfaces and non-equilibrium structures generated using coordinate randomization and ab-initio molecular dynamics of the equilibrium structures. The initial database is used to construct an initial interatomic potential model which is then used to perform molecular dynamics simulations to generate additional non-equilibrium structures. The interatomic potential is improved though an active learning process by evaluating its performance based on (1) accuracy, (2) stability, and (3) reliability [8]. The accuracy is measured based on the energy and force mean square errors and root mean square errors with respect to the DFT calculations. On the other hand, the stability is monitored by checking for any exploding atoms or formation of unphysical structures. This can also be quantitatively checked by looking for any sharp changes in total energy and simulation temperature. Finally, the reliability is determined based on sufficiency of the atomic environment in the database. This will be discussed further in the next section.

The active learning process allows the addition of new structures with atomic environments that are not represented in the database. The fine-tuning and evaluation of the interatomic potential is continued until all the three criteria have been satisfied. These process is outlined in Fig. 1.

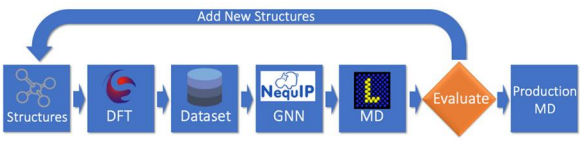

Fig. 1. Graph Neural Network interatomic potential construction, fine-tuning, and evaluation.

3.2. Reliability Estimation

The reliability is estimated based on the presence or absence of atomic environment on the database similar to the atomic environments that appear during the molecular dynamics simulations. Machine learning of interatomic potential is a kind of regression modelling. Therefore, the predictions are more reliable in interpolating between datapoints and less reliable in extrapolating. We determine the extrapolated atomic environment based on the feature vectors calculated using graph message passing, where the aggregate function or convolution is calculated using the product of Bessel radial function $R(r_{ij})$ and spherical harmonics $Y_m^l(\hat{r}_{ij})$:

$$AGGREGATE = tanh\left(\sum_{i\neq j}^{N} R(r_{ij}) f(r_{ij}, r_c)\, Y_m^l(\hat{r}_{ij})\right) \quad (1)$$

$$R(r_{ij}) = \frac{2}{r_c}\frac{\sin\left(\frac{b\pi}{r_c} r_{ij}\right)}{r_{ij}}\, f(r_{ij}, r_c) \quad (2)$$

$$f(r_{ij}, r_c) = 1 - \frac{(p-1)(p+2)}{2}\left(\frac{r_{ij}}{r_c}\right)^p + p(p+2)\left(\frac{r_{ij}}{r_c}\right)^{p+1} - \frac{p(p+1)}{2}\left(\frac{r_{ij}}{r_c}\right)^{p+2} \quad (3)$$

Here, $f(r_{ij}, r_c)$ is a polynomial cutoff function which ensures smooth the decay of the radial function at the cutoff radius r_c. The details of this method are discussed in our recent publication [8].

To illustrate this concept, we plot the 2-dimensional projection of the feature vector of the entire database (black) using TSNE method in Fig. 2. Using the TSNE method, the feature vectors were clustered based on their similarities. Next, we plotted the feature vectors corresponding to the atoms in equilibrium and slightly perturbed equilibrium structures (SPES) of diamond bulk (blue), graphite (orange), and surface atoms of the C(100) (violet) and unreconstructed (green) and reconstructed (red)

C(111) surfaces. These structures occupy the clusters on the plot. In Figure 3a, we plotted the same feature vectors with the addition of the feature vectors corresponding to the sublayers of the C(100) and C(111) surfaces. We can see that most of the clusters of atomic environments have been identified. The remaining unidentified atomic environments shown by small clusters and cluster boundaries correspond to the reactive or transition state structures from one equilibrium state to another. The extrapolated atomic environment will appear on the plot as isolated dots or dots in between clusters. The lack of neighboring atomic environments means that energy and force predictions for the extrapolated atomic environments are likely unreliable. The extrapolated atomic environments are then added to the database and will be included in the training of the next version of the interatomic potential.

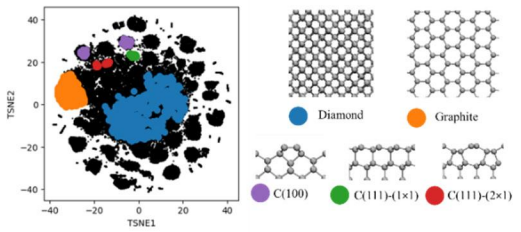

Fig. 2. Plot of feature vectors of the structures on the database projected in 2D space (black) with the feature vectors corresponding to diamond (blue), graphite (orange), and the surface atoms of the C(100) (violet), unreconstructed C(111) (green), and reconstructed C(111) (red) surfaces.

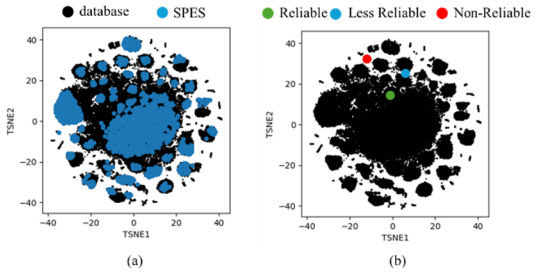

Fig. 3. (a) Plot of feature vectors of the structures on the database projected in 2D space (black) with the feature vectors corresponding to slightly perturbed equilibrium structures (SPES) (blue). (b) Regions containing atomic environments classified as reliable, less reliable, and non-reliable.

3.3. Hybridization Analysis Using Neural Network Binary Classifier Model

Molecular simulation data of covalent solids like diamond and silicon usually employs coordination analysis for structure identification and characterization. Using this method, 1- and 2-coordinated atoms are classified as sp^1 hybridized, and the 3- and 4-coordinated atoms are classified as sp^2 and sp^3 hybridized, respectively. However, sp^3-hybridized atoms can also be 3-coordinated when there is a dangling bond. Since the properties of sp^2 and 3-coordinated sp^3 atoms are not the same, it is necessary to distinguish between the two type of atoms. For this purpose, we constructed a supervised binary classifier neural network model where we used a database of slightly perturbed sp^2 and 3-coordinated sp^3 hybridized atoms from graphite and diamond surfaces, respectively, with the bond lengths and bond angles as learning representation. Figure 4 implements this analysis on the thermally degraded C(111) and C(100) surfaces [8]. The proportion of sp^2 and 3-coordinated sp^3 atoms in the thermally degraded C(111) surface is almost similar. In comparison, the proportion of 3-coordinated sp^3 atoms in the thermally degraded C(100) surface is significantly higher compared to the sp^2 atoms. This analysis implies that the thermally degraded atoms on the C(111) and C(100) surface are expected to have different properties.

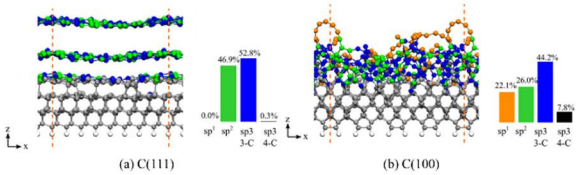

Fig. 4. Comparison of the hybridization of the thermally degraded atoms on the C(111) and C(100) surfaces [8].

3.4. Detection and Analysis of Chemical Reactions on the MD Simulation Using Feature Vectors

Analysis of MD trajectory will generate new physical and chemical insights. However, isolating individual chemical reactions is very challenging, especially for large scale MD simulations. Here, we propose a method of detecting chemical reactions by monitoring the changes in atomic or chemical environments which in turn are represented by changes in feature vectors calculated by graph message passing. For instance, during a simulation where there is no ongoing chemical reaction, the feature vector has to be constant. When a chemical reaction happens, an inflection in the feature vector plot must occur. We illustrate this concept in Figure 5. We choose a central atom (grey sphere with red highlight) and plot the radial component of the feature vector. The plot from structures A-C shows the metastable adsorption of O_2 on top of the C(100) surface, C-D shows the O_2 metastable adsorption transforming to O_2 molecular adsorption, and D-E shows the O_2 dissociation and C-dimer bond breaking. The structures A, B, C, D, and E all coincide on the inflection points on the plot. The two inflection points between A and B are caused by the O_2 adsorption on the neighboring atoms of the central atom.

4. Conclusion

We constructed a machine learning interatomic potential based on graph neural network model for the investigation of diamond surface oxidation and thermal degradation. In this paper, we presented the active learning method of database and interatomic potential construction and fine tuning. In this active learning method, we evaluated the interatomic potential based on accuracy, stability, and reliability. The reliability can be estimated by detecting extrapolated atomic environments that may arise during the MD simulation. We also presented the use of neural network binary classifier trained using bond lengths and bond angles as descriptors to differentiate between sp^2 and sp^3-hybridized atoms in simulating diamond surfaces. These method gave insights that augment the conventional coordination analysis. Finally, we propose the use of feature vectors calculated using graph message passing in the detection and analysis of chemical reactions during MD simulations. The changes in the plot of feature vector component over time have been shown to indicate a change in chemical environment and the inflection points coincide with equilibrium and metastable structures.

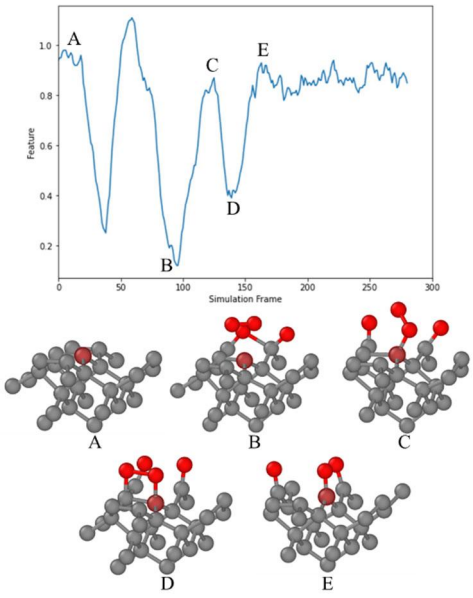

Fig. 5. Plot of the radial component of the feature vector of central atom (grey sphere with red highlight) vs the simulation frame, showing the changes in chemical environment:

References

[1] Wort and Balmer Materials Today **11**, 1–2 (2008)

[2] Prawer and Greentree Science **320**, 5883 (2008)

[3] Toros et al. Diam. and Rel. Mat. **108**, 107839 (2020)

[4] Nagai et al. Sci Rep **8**, 1 (2018)

[5] STATE Code, www-cp.prec.eng.osaka-u.ac.jp/puki_state/

[6] Batzner et al. Nat. Commun **13**, 1 (2022)

[7] Thompson et al. Comput. Phys. Commun. **271**, 108171 (2022)

[8] Enriquez et al. Carbon (2024) In press. https://doi.org/10.1016/j.carbon.2024.119223